Available online at www.sciencedirect.com

SCIENCE DIRECT®

ELSEVIER

International Journal of Heat and Mass Transfer 48 (2005) 2868–2877

International Journal of HEAT and MASS TRANSFER

www.elsevier.com/locate/ijhmt

Critical heat flux performance for flow boiling of R-134a in vertical uniformly heated smooth tube and rifled tubes

Chang Ho Kim *, In Cheol Bang, Soon Heung Chang

Korea Advanced Institute of Science and Technology, 373-1, Guseong-dong, Yuseong-gu, Daejeon 305-701, Republic of Korea

Received 10 December 2004; received in revised form 25 January 2005
Available online 22 April 2005

Abstract

In the present paper, critical heat flux (CHF) experiments for flow boiling of R-134a were performed to investigate the CHF characteristics of four-head and six-head rifled tubes in comparison with a smooth tube. Both of rifled tubes having different head geometry have the maximum inner diameter of 17.04 mm while the smooth tube has the average inner diameter of 17.04 mm. The experiments were conducted for the vertical orientation under outlet pressures of 13, 16.5, and 23.9 bar, mass fluxes of 285–1300 kg/m^{2}s and inlet subcooling temperatures of 5–40 °C in the R-134a CHF test loop. The parametric trends of CHF for the tubes show a good agreement with previous understanding. In particular, CHF data of the smooth tube for R-134a were compared with well-known CHF correlations such as Bowring and Katto correlations. The CHF in the rifled tube was enhanced to 40–60% for the CHF in the smooth tube with depending on the rifled geometry and flow parameters such as pressure and mass flux. In relation to the enhancement mechanism, the relative vapor velocity is used to explain the characteristics of the CHF performance in the rifled tube.

Keywords: R-134a; Critical heat flux; CHF enhancement; Rifled tube; Ribbed tube

1. Introduction

Critical heat flux (CHF) is the heat flux at which boiling crisis occurs and a sudden deterioration of heat transfer rate occurs, and sets a limit in designing and operating the boiling heat transfer equipments in power industry such as nuclear, fusion and fossil power plants. Thus any increase in the critical heat flux can increase the safety margins and allows the economic design and operation at higher heat fluxes.

In recent years, the requirements for coal-fired power plants lead to a change in operating mode from constant to variable pressure [1]. The combined requirement of higher efficiency and more operating flexibility in intermediate peaking and peak load duty resulted in the implementation of once-through boiler with suitability for variable-pressure operation. The development of once-through evaporator concepts with vertical tubes began in the 1980s. The low mass flow vertical tube furnace design in once-through evaporator allows variable pressure operation, on/off cycling, and rapid load change. The success of the low mass flow vertical tube with variable pressure design depends on the capability

* Corresponding author. Tel.: +82 42 869 3856; fax: +82 42 869 3810.

E-mail addresses: hokim4@kopec.co.kr (C.H. Kim), musoyou@kaist.ac.kr (I.C. Bang), shchang@kaist.ac.kr (S.H. Chang).

0017-9310/$ - see front matter
doi:10.1016/j.ijheatmasstransfer.2005.01.039

Nomenclature

a_r	centrifugal acceleration (m/s^2)
D	inside diameter (m)
L	lead length in rifled tube(m)
LHS	left hand side
g	gravity acceleration (m/s^2)
N	number of ribs
P	pitch length in rifled tube (m)
q_c	critical heat flux (kW/m^2)
R	inside radius in rifled tube (m)
RHS	right hand side
V_a	axial velocity (m/s)
V_{gf}	relative vapor velocity (m/s)
V_r	tangential velocity (m/s)
w	rib width in rifled tube (m)
Greek symbols	
ρ	density of fluid (kg/m^3)
σ	surface tension (N/m)
θ	acceleration ratio
φ	helical angle of rib
Subscripts	
f	saturated liquid
g	saturated vapor

of the tube internal geometry to promote cooling of the tube when exposed to high heat fluxes.

Therefore, a lot of advanced cooling techniques have been considered for increasing not only heat transfer but also the CHF in the boiler tube. In particular, the CHF in the forced-convection boiling tubes depends on the wetting condition of the tube inside wall. Beginning at a certain percentage of steam quality, the smooth tube walls can no longer be kept completely wetted and the heat transfer is sharply reduced at the unwetted tube wall. It is well known that a swirl flow, which makes the tube wall more wetted, can significantly improve the CHF as well as the heat transfer coefficients in the forced convection boiling tube. The increases in CHF are commonly in the range of 50–100% and depend on swirl generation method and geometry of devices. Swirl flow in tubes may be classified into two essential types: continuous swirl flow and decaying swirl flow. The swirling motion in continuous swirl flow is maintained over the whole length of tube, while the swirl in decaying swirl flow is generated at the swirl generation device and decays along the flow path. Swirl flow is generally generated by twisted types, propellers, vortex generator, coiled wire and rifled tubes.

In particular, it has been reported in lots of literatures [2–8] that the rifled tube reveals the significant improvement in heat transfer and critical heat transfer. However, the degree of improvement depends greatly on the geometry of the rifle on the inner surface of the tube. The improvement has been explained by a centrifugal action at the fluid flowing near the surface. The ribs have the water near wall be rotated to generate a swirl flow. This results in a centrifugal action which forces the water to the tube wall, retards re-entrainment of the liquid, and causes the drift on the radial direction to carry the vapor to the centre. The steam blanketing and film dryout at CHF conditions are thus prevented until substantially higher steam qualities are reached.

Zarnett and Charles [9] investigated the two-phase flow patterns and their works indicated that swirl flow was not obtained until a critical liquid superficial velocity was reached. Weisman et al. [10] studied the two-phase flow patterns in the presence of helical wire ribs with the helical angle of 37°–58° and proposed that a CHF enhancement in rifled tube would occur above the minimum liquid velocity. The work of Watson et al. [11] showed that the critical mass flux should be exceeded to obtain the CHF enhancement in rifled tube. It is clear from these investigations that the swirl flow is related to CHF enhancement in the forced convective boiling condition.

Cheng and Xia [8] conducted the CHF experiments in the smooth tube and a four-head rifled tube with helical angle of 40° to investigate the effects of mass flux and pressure on CHF enhancement. While their test results showed that CHF in rifled tube was enhanced by a factor of 1.3–1.5 and no CHF increases at near critical pressure in rifled tube, no mechanistic explanation was provided in their study. Nishikawa et al. [3] showed that the internally helical grooved tube prevented film boiling occurring until higher steam quality compared to the smooth tube. The critical qualities depended greatly on the geometric type of the grooved tube, working pressure, mass flux, and the heat flux.

Kohler and Kastner [6] investigated the effect of the internal rifling on heat transfer and assessed the effectiveness of the rib by means of an acceleration ratio which corresponds to the ratio of centrifugal acceleration to acceleration due to gravity. Their investigation showed that the heat transfer in rifled tube was considerably enhanced at near the critical pressure.

The swirl effect is generally quantified as the ratio of centrifugal acceleration to the gravity as follows:

$$\theta = \frac{a_r}{g} = \frac{V_r^2}{Rg} = \frac{V_a^2}{Rg\tan(\varphi)^2} \tag{1}$$

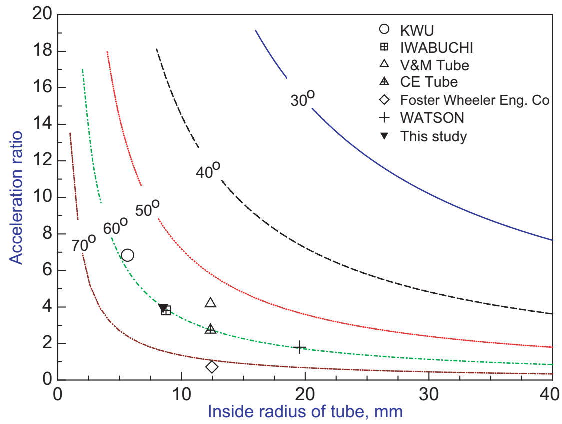

Fig. 1. Acceleration ratio of rifled tubes [6].

This equation means that the centrifugal acceleration is a function of only one variable, helical angle at the given inside diameter. Fig. 1 [6] shows the relationship between helical angle and acceleration ratio, and the acceleration ratios for the tubes used in the boiler manufacturers. As is apparent from Fig. 1, the lower helical angle results in the greater acceleration ratio, which means the greater CHF enhancement. Since most of rifled tubes have the helical angle of around 60°, this study uses the rifled tube with 60° helical angle to investigate the CHF characteristics of rifled tube.

The effectiveness for the rifled tubes to enhance the critical heat transfer rate has close relations with their internal configuration since their internal surface contacts directly the fluid to generate the swirl. The stronger is the swirl effect of the internal ribs, the more effective is the rifled tubes to enhancement the critical heat transfer rate. The geometric shape of the ribs in the rifled tube can be generally determined by seven parameters; inside diameter (D), helical angle (φ), number of rib (N), rib width (w), lead (L), pitch (P) and rib height (h). The inside diameter, lead, helical angle, number of rib and pitch are related as follows:

$$\text{Lead},\ L = \pi D \tan(\varphi) \tag{2}$$

$$\text{Number of rib},\ N = L/P \tag{3}$$

Therefore, four independent parameters define the shape of rib except for the inside diameter, which is given from the integrated system design. Among the four parameters (number of ribs, height, helical angle and width), only a helical angle was considered in the centrifugal acceleration ratio as defined in Eq. (1).

The experimental results reported in literature show that the other geometric parameters are an important factor on the flow pattern and the boiling heat transfer characteristics [3,10,16]. However, any quantification on the effectiveness of the rib to generate the swirl and enhance the CHF in the rifled tube has not been proposed from literature.

Despite the experimental works carried out to investigate the convective boiling heat transfer characteristics in rifled tube because of the important effect of ribs in boiler design, it is apparent that detailed investigations have not been widely known from literature. Also, these investigations just compared the wall temperatures of rifled tube and a smooth tube in boiling crisis. The more comprehensive study on CHF in the rifled tubes would be desirable.

The main purpose of the study is to improve our understanding on CHF characteristics of the boiler rifled tube generating a passive swirl flow through CHF experiments in the vertical smooth tube and rifled tubes. As a working fluid, R-134a was selected to replace other refrigerants banned due to their destruction of the ozone layer and for the high pressure-high temperature simulation of a water-cooled system [15]. The investigation results can be used to provide additional physical insight for some of CHF enhancement mechanism in rifled tubes.

2. Experimental apparatus and procedure

2.1. Experimental loop

The CHF experiments were performed in Korea Advanced Institute of Science and Technology (KAIST) R-134a CHF test facility as shown in Fig. 2 [15]. The R-134a experimental loop consists of the following components: a test section as a test tube, a mass flow meter, a pre-heater for inlet subcooling control, an accumulator for pressure control, a canned pump for stable mass supply, a condenser, and a chilling system with R-22 and water-propylene glycol. An adjusting valve is used to precisely control flow rate to the test section. The loop is filled with R-134a in the vacuum condition. The test loop is designed for pressure of 30 bar and 200 °C. The loop flow is measured by the mass flowmeter calibrated to be 2% of RMS error by manufacturer. Temperatures and pressures are measured at various locations as indicated by T and P, respectively, in Fig. 2.

2.2. Test section

The test section is schematically shown in Fig. 3(a) and is carbon steel (SA182) tube with upward flow. The tube is electrically heated directly with a DC power supplier, which controls the power by a power transformer with silicon controlled rectifiers (SCRs) with the maximum power capacity of 40 V and 5000 A. The maximum heated length of test section is 3000 mm and the heated length is reduced by adjusting

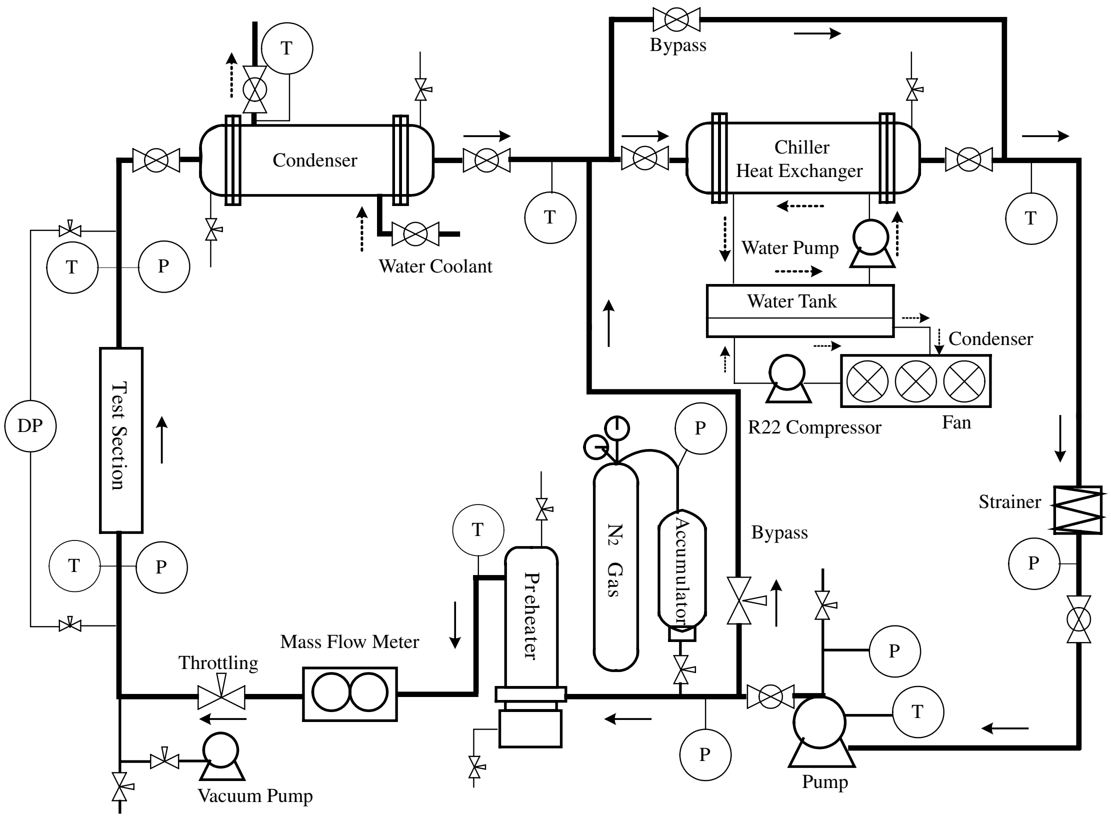

Fig. 2. Schematic diagram of the experimental system [15]. P: Pressure instrumentation; T: Temperature instrumentation; DP: Differential pressure instrumentation.

the position of the upper power terminal in order to investigate the heated length effect on the CHF. The smooth tube has an inner diameter of 17.04 mm. The rifled tubes have the maximum inside diameter of 17.04 mm. The detailed geometrical information of the testing tubes is summarized in Table 1. Fig. 3(b) shows the axial-sectional pictures of the rifled tubes and the geometric parameters of ribs in rifled tube. The temperatures of the liquid at the inlet and outlet of the test section are measured with the in-stream T-type sheathed thermocouples. The temperatures of the outside wall are measured at 20 locations along the channel wall, and two K-type thermocouples are installed at each location. The first two thermocouples are located 5 mm below from the end of upper power clamp. Outlet pressure and inlet pressure are measured with pressure transducers and calibrated to be 0.5% of RMS error for a full range.

A pair of clamp type copper electrodes grabbed both ends of the test tube. Test section is connected to the flange, which is insulated from other part of the test loop by Teflon. The supplied current and the voltage difference between both ends of the test section are measured and collected by a data acquisition system.

2.3. Test procedure and test matrix

The flow direction is vertically upward. For all test conditions, the CHF data were taken. All process data including the tube wall temperatures were collected by a data acquisition system for later analysis. Before each series of experiments, a heat balance test was performed and showed that the heat losses were within 2.5%. First, the pump starts and the mass flow is controlled by the speed control with the converter and the control valve at a certain level. The test pressure in the test loop is increased by turning on the pre-heater and continuously increasing its power. After the pressure in the test loop reaches a pre-determined level, the inlet temperature is controlled by the power control to the pre-heater. The power to test section is increased at first rapidly to about 85% of CHF and then slowly. When the power is supplied to test section, the system pressure is controlled by venting the nitrogen gas in two accumulators. Boiling crisis is considered to occur when the wall temperature just below the upper power terminal is suddenly increased.

Table 2 summarizes the test matrix and the equivalent water-based conditions. The test conditions are

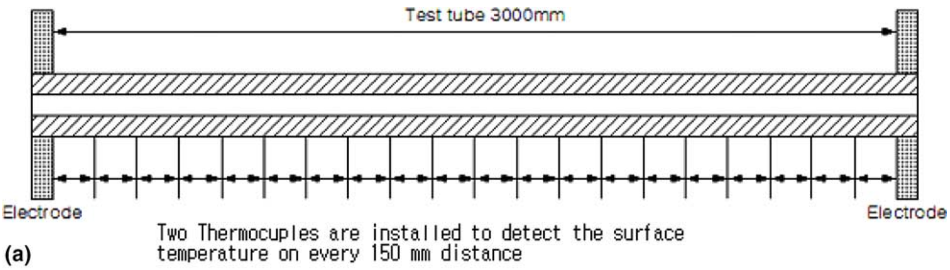

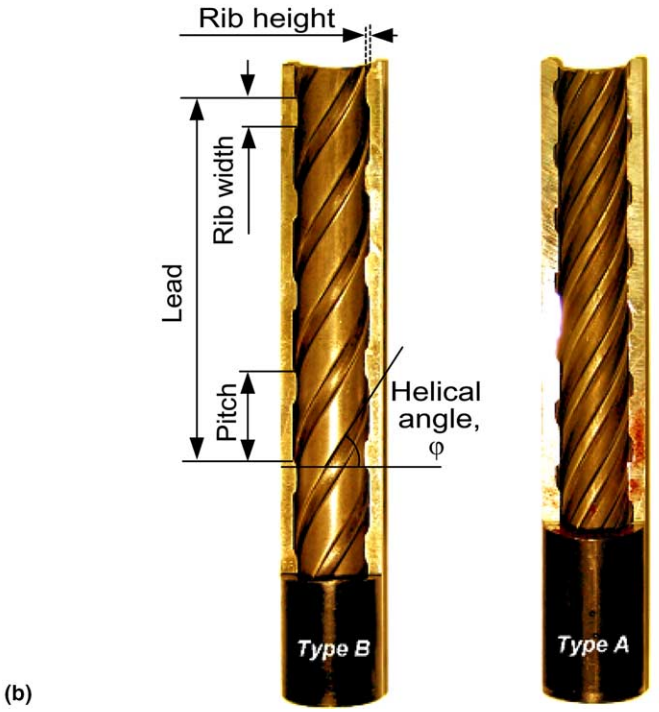

Fig. 3. Test section and rifled tube. (a) Schematic diagram of test section and (b) cross-sectional view of the rifled tubes and their geometric parameters.

Table 1
Geometric dimensions of testing tubes

Tube type	OD, mm	ID_{min}, mm	Rib height, mm	No. of ribs	Width, mm	Helical angle	Pitch, mm
Smooth	22.59	17.04	N/A	N/A	N/A	N/A	N/A
Type B	22.59	15.22	0.91	4	5.59	60	23.19
Type A	22.59	15.34	0.85	6	8.28	60	15.46

selected by considering the startup condition of an evaporator of a fossil power plant and the capacity of KAIST test loop. The inlet subcooling temperatures are 5–40 °C. The CHF test in the rifled tubes was performed under the specific test conditions not exceeding the limitation of the power capability because of their very high CHF values.

3. CHF test results and discussion

3.1. Smooth tubes

Fig. 4(a) and (b) show the effect of the inlet subcooling enthalpy on CHF at different flow conditions in the smooth tube. The results are obtained at the pressures of

Table 2
Test matrix

Test matrix condition in R-134a and their water-equivalent conditions								
Pressure (bar)		Saturated temperature, °C		Mass Flux (R-134a), kg/m^2 s				
				285	500	712	1000	1300
R-134a	Water	R-134a	Water	Mass flux (water), kg/m^2 s				
13	70	49.4	295	402.1	705.4	1004.5	1410.8	1834.0
16.5	100	59.2	311	400.4	702.4	1000.2	1404.8	1826.3
23.9	140	75.5	336.6	396	695.3	990.1	1390.6	1807.7

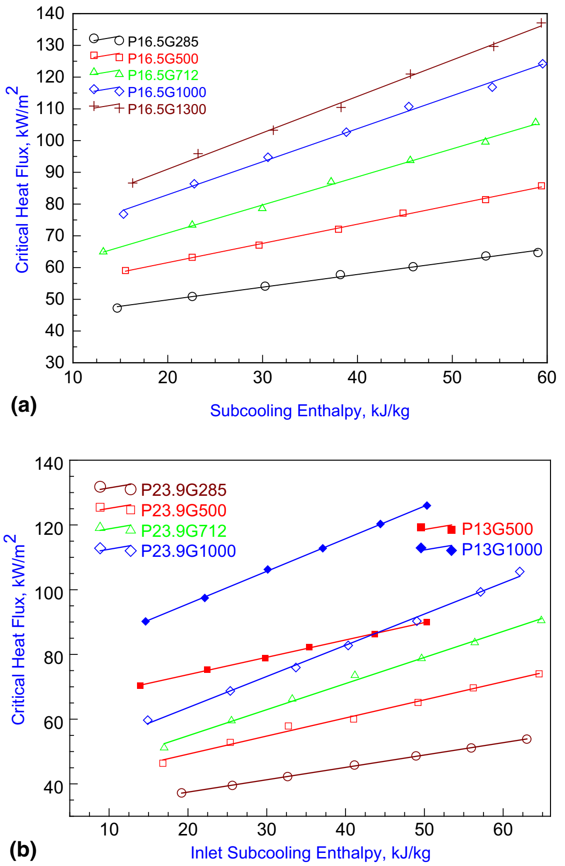

Fig. 4. Effect of inlet subcooling enthalpy on CHF of R-134a in vertical smooth tube. (a) Outlet pressure: 16.5 bar and (b) outlet pressures: 13 bar and 23.9 bar.

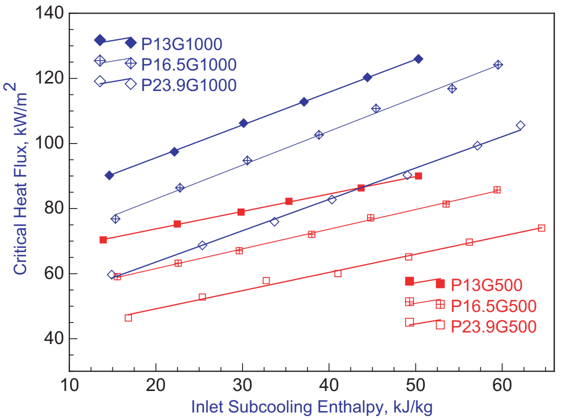

Fig. 5. Effect of system pressure on CHF of R-134a in vertical tube ($G = 500$ & 1000 kg/m^{2}s).

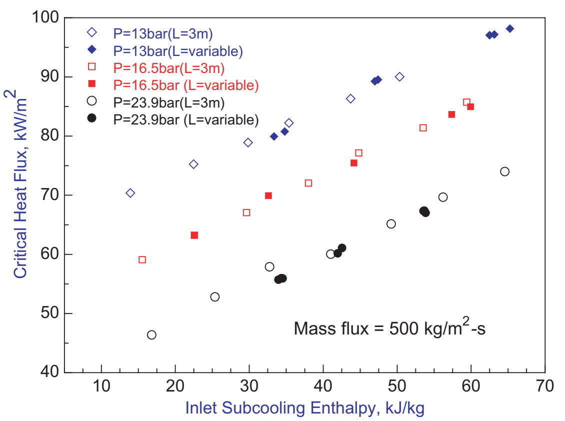

Fig. 6. Effect of the heated length on CHF in the smooth tube.

13, 16.5 and 23.9 bar and at the mass fluxes of 285, 500, 712, 1000 and 1300 kg/m^{2}s. The CHF increases almost linearly with the inlet subcooling enthalpy, but the effect decreases with decreasing mass flux. Fig. 5 shows the effect of the pressure on CHF, indicating that CHF decreases with increasing the pressure. Fig. 6 shows the heated length effect on the CHF after converting the inlet subcooling enthalpy to the equivalent heated length of 3 m. The adjustment is accomplished by lowering the inlet enthalpy by an added heat across the extra heated length. It indicates that linear CHF-inlet subcooling enthalpy relationship is maintained regardless the heated length over the investigated length of 2–3 m.

For comparing with the present experimental data, two different prediction methods are used: (1)

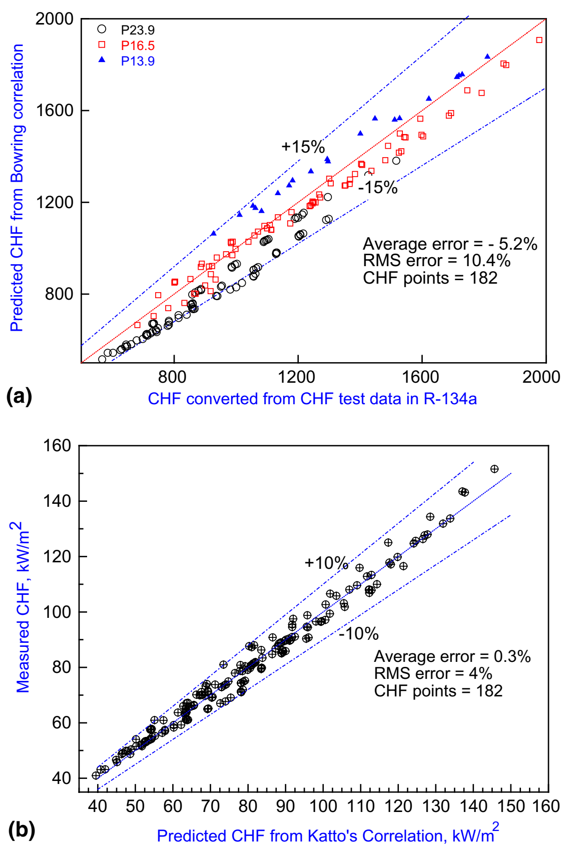

Fig. 7. Comparison of test results in vertical tube with (a) Bowring and (b) Katto correlations.

correlation of Bowring [17] and (2) generalized correlation of Katto [18] because these correlations are known as good prediction methods covering a wide range of flow conditions and tube geometry.

Since this correlation is applicable for only water, the present CHF data of R-134a are first converted into water-equivalent values using thermal-physical properties of the water and R-134a. 182 data points are used for comparison with the prediction method. Fig. 7(a) shows the comparison of the water-equivalent CHF data converted from the CHF data in R-134a with the CHF prediction using Bowring correlation. The RMS error and average error of the prediction are 10.4% and −5.2%, respectively. A good agreement is achieved between the converted CHF and the predicted CHF. A systematical analysis reveals that the calculated CHF generally underestimates the CHF test results and the deviation depends on the system pressure. For 13, 16.5 and 23.9 bar, the average errors of the prediction CHF are 5.2, −4.1 and −12.9%, respectively. It agrees with the CHF investigation in R-134a of Tain and Cheng, presented that for the high pressure the CHF prediction using fluid-to-fluid modeling resulted in under-prediction of CHF [13].

Fig. 7(b) shows the comparison of CHF test data in R-134a with the CHF data obtained by using the generalized correlation of Katto. The RMS error and average error of the prediction are 4% and +0.3, respectively. A very good agreement is achieved between the CHF test data and the predicted CHF data. A systematical analysis reveals that there is no dependency on the system pressure. Katto presented that there were four characteristic regimes of CHF, called L-, H-, N-, and HP-regime, where L-regime is the regime mainly corresponding to the dryout, N-regime is the regime mainly corresponding to the departure from nucleate boiling (DNB), H-regime is the intermediate regime between L- and N-regime, and HP-regime is a special regime when the system pressure is extremely high [12,14]. Fig. 8 shows that all experimental data investigated in this study belongs to H-regime except for the CHF data obtained at the pressure 23.9 bar with the mass flux 1300 kg/m^{2}s. These data correspond to N-regime. It is ascertained that most of CHF data belongs to the dry-out-type CHF except that a few of CHF data investigated at 23.9 bar belongs to DNB type.

3.2. Rifled tubes

Experiments of CHF were performed for the rifled tubes (Type A and B) to compare the CHF values. The data are plotted against the inlet subcooling enthalpy, mass flux and outlet pressure.

Fig. 9 shows the CHF vs. ΔH_{sub} graph for the four primary flow conditions ($G = 285$, 500, 712 and 1000 kg/m^{2}s) and pressure of 16.5 bar in the rifled tubes (Type A and B). This figure presents that the CHF increases almost linearly with the inlet subcooled enthalpy for both types of rifled tubes. Fig. 10 shows the CHF vs.

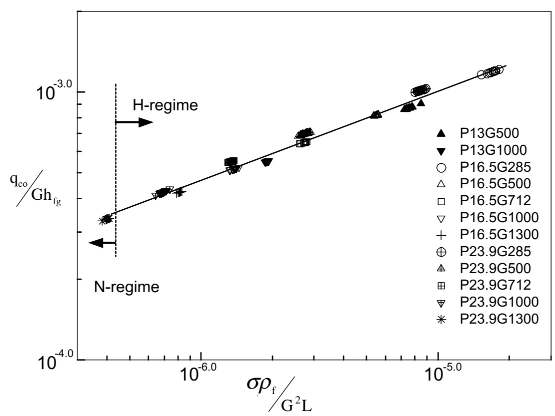

Fig. 8. CHF characteristics of R-134a (H-regime and N-regime).

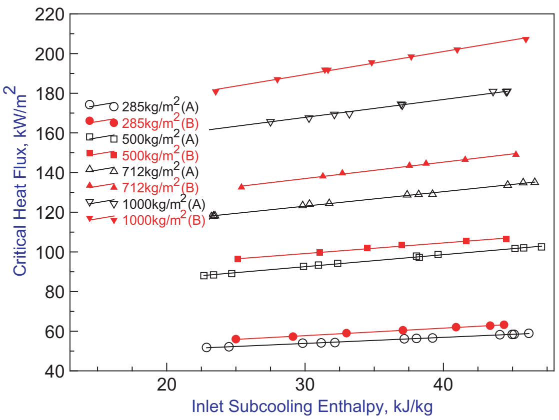

Fig. 9. Effect of inlet subcooling enthalpy on CHF of R-134a in rifled tubes (outlet pressure: 16.5 bar).

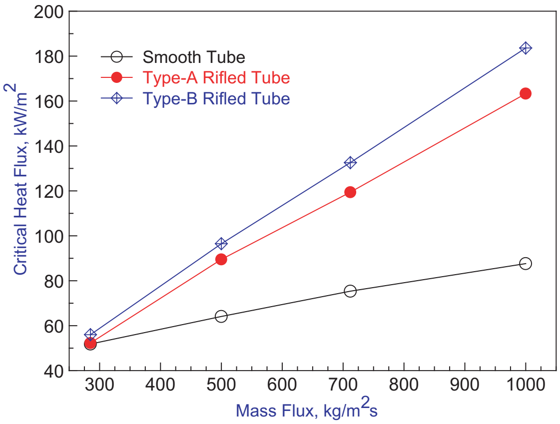

Fig. 10. CHF vs. mass flux for one smooth tube and two rifled tubes at 16.5 bar.

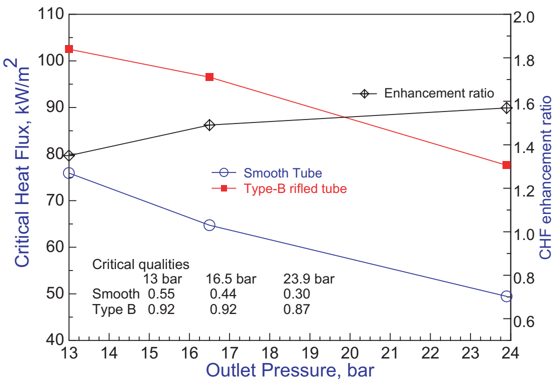

Fig. 11. CHF vs. outlet pressure at the mass flux of 500 kg/m^{2}s.

mass flux for the inlet subcooling enthalpy of 25 kJ/kg and pressure of 16.5 bar in one smooth tube and two rifled tubes. The parametric trends of CHF of R-134a in the rifled tubes are similar with that in the smooth tube. As shown in Fig. 10, the CHF increases with increasing mass flux regardless of tube type and the CHF enhancement in the both rifled tubes depends on the mass flux and is much pronounced with increasing the mass flux. It can be explained by the increased swirl effect due to the increase of the tangential velocity near the rib. At the low mass flux of 285 kg/m^{2}s, no significant CHF enhancement is shown in the rifled tubes compared to the smooth tube. It agrees with other investigations [9–11] where the critical mass flux is required to get the CHF enhancement in the rifled tube. Fig. 11 shows that CHF vs. outlet pressure for the inlet subcooling enthalpy of 25 kJ/kg and mass flux of 500 kg/m^{2}s. The CHFs in both tubes decreases with increasing the pressure, but the enhancement ratio in the rifled tubes increases to some degree with increasing the pressure. This trend seems to be in contradiction to the general understanding of the vapor drift under the centrifugal acceleration field because the drift force decreases with increasing the pressure due to decreasing the density difference between the vapor and liquid and its reduction makes the CHF enhancement in the swirl flow weak. But, it can be explained by the factor that the CHF enhancement in the rifled tube is achieved by extending the nucleate boiling region to the higher quality. As shown in Fig. 11, while the critical quality of the rifled tube is not significantly affected by the pressure, the critical quality in the smooth tube is relatively more affected. The amount of critical quality extended due to the swirl effect in the rifled tube is increased with increasing the pressure and results in the CHF enhancement. The above CHF enhancement ratio trend against the pressure can be explained by considering both opposite effects.

Fig. 12 shows the CHF vs. ΔH_{sub} graph for the Type-B rifled tube with the various heated length. It indicates that linear CHF-inlet subcooling enthalpy relationship is maintained regardless the heated length over the investigated length of 2–3 m.

Based on these test results and the literature survey, the CHF characteristics in the rifled tube can be summarized as follows:

- The CHF enhancement in the rifled tube depends on the mass flux and pressure.
- The critical velocity (or mass flux) shall be exceeded to get the CHF enhancement.
- The CHF enhancement ratio increases with increasing the mass flux.
- With increasing the pressure, the CHF enhancement ratio increases and disappears near the critical pressure [7,8].
- There are a critical helical angle to get the CHF enhancement [6].

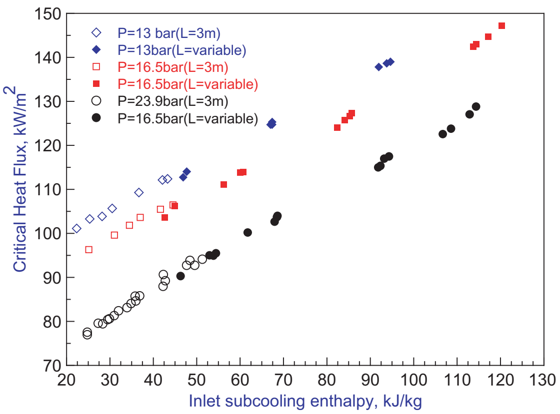

Fig. 12. CHF vs. inlet subccoling enthalpy to show the effect of the heated length on CHF in the Type-B rifled tube.

The swirling motion forces the vapor in the liquid film to the centre of the tube. Therefore, the characteristics of the CHF enhancement in the rifled tube can be explained by the relative velocity of vapor under the centrifugal acceleration due to the swirl flow. Based on the drift-flux model of two-phase flow, the relative vapor velocity due to the centrifugal acceleration field can be defined as [10]:

$$V_{\mathrm{gf}} = k\left[\frac{(\rho_{\mathrm{f}}-\rho_{\mathrm{g}})\sigma a_r}{\rho_{\mathrm{f}}^2}\right]^{1/4} = k\left[\frac{(\rho_{\mathrm{f}}-\rho_{\mathrm{g}})\sigma}{\rho_{\mathrm{f}}^2}\right]^{1/4} \times \left[\frac{V_{\mathrm{a}}^2}{Rg\tan(\varphi)^2}\right]^{1/4} \quad (4)$$

If the relative vapor velocity is reduced below a particular value, it would be expected that flow ceases to follow the ribs and the centrifugal acceleration decreases. In this situation, the CHF enhancement due to rifled tube would not exit. The parametric trends of the relative vapor velocity on the pressure, helical angle and velocity can be summarized as follows:

- The value of the first term in RHS rapidly decreases near the critical pressure.
- The value of the second term in RHS rapidly decreases above the helical angle of 70° and below the velocity of 0.3 m/s.

Actually in this study, the mass flux of 285 $\mathrm{kg/m^2 s}$ corresponds to the liquid velocity of around 0.27 m/s at 16.5 bar. The higher mass flux results in the higher liquid velocity and consequently the greater centrifugal acceleration. These factors supports that the relative vapor velocity due to the centrifugal acceleration field is strongly related to the CHF enhancement mechanism.

The type-B rifled tube has a superior performance in the CHF compared to the type-A for all test conditions. It indicates that except the helical angle and rib height, the other geometric parameters (the rib number and the rib width) are the important factors on the boiling heat transfer characteristics. Further research work needs to quantify the relationship between the CHF enhancement and the geometric parameters of ribs in the rifled tube.

4. Conclusion

Experiments for critical heat flux using R-134a in one vertical smooth tube and two rifled tubes were performed. Based on this investigation, the following conclusions are obtained.

(1) A CHF predicted from Bowring correlation results in a good agreement with the water-equivalent present CHF data. A very good agreement is achieved with Katto correlation regardless of the flow conditions. Based on the characteristic regimes of CHF, it may be presumed that most of CHF data belongs to the dryout-type CHF except that a few of CHF data investigated at 23.9 bar belongs to DNB type.
(2) The parametric trends of CHF of R134a in the rifled tubes are similar with that in the smooth tube.
(3) The CHF characteristics in the rifled tube can be summarized as follows:
   - The CHF enhancement in the rifled tube depends on the mass flux and pressure.
   - There are a critical helical angle and the critical velocity (or mass flux) to get the CHF enhancement.
   - The CHF enhancement ratio increases with increasing the mass flux.
   - With increasing the pressure, the CHF enhancement ratio increases and disappears near the critical pressure.
(4) The characteristics of the CHF enhancement in the rifled tube was explained by the relative velocity of vapor under the centrifugal acceleration due to the swirl flow. The parametric trends of the relative vapor velocity on the pressure, helical angle and velocity can be summarized as follows:
   - The value of the first term in RHS rapidly decreases near the critical pressure.
   - The value of the second term in RHS rapidly decreases above the helical angle of 70° and below the velocity of 0.3 m/s.
   - These factors supports that the relative vapor velocity due to the centrifugal acceleration field is strongly related to the CHF enhancement mechanism.

(5) The type-B rifled tube has a superior performance in the CHF compared to the type-A for all test conditions. It indicates that except the helical angle and rib height, the other geometric parameters (the rib number and the rib width) are the important factors on the boiling heat transfer characteristics. Further research work needs to quantify the relationship between the CHF enhancement and the geometric parameters of ribs in the rifled tube.

Acknowledgements

This work was sponsored by Doosan Heavy Industries and Construction Co., Ltd. and the "*National Laboratory*" program of the Korean Ministry Of Science and Technology (MOST). The authors would like to express their appreciation to Dr. Y.H. Jeong of KAIST, to Dr. S.Y. Chun and Dr. S.K. Moon of KAERI, and to Mr. Y.S. Kim, O.C. Yang, and Dr. J.J. Yun of DHI.

References

[1] S. Kakac (Ed.), Boilers, Evaporators, and Condensers, Wiley-Interscience, 1991.
[2] P.B. Whalley, The effect of swirl on critical heat flux in annular two-phase flow, Int. J. Multiphase Flow 5 (1979) 211–217.
[3] Nishikawa et al., Improvement in heat transfer performance at high heat fluxes with internally grooved boiler-tubes, Memoirs of the faculty of engineering, Kyushu university, vol. 35(2), December 1975.
[4] L. Cheng, T. Chen, Flow boiling heat transfer in a vertical spirally internally ribbed tube, Heat Mass Transfer 37 (2001) 229–236.
[5] M. Iwabushi et al., Heat transfer characteristics of rifled tubes in near critical pressure region, in: Proc. 7th Int. Heat Transfer Conf., Munich, vol. 5, 1982, pp. 313–318.
[6] W. Kohler et al., Heat transfer and pressure loss in rifled tubes, in: Proc. 8th Int. Heat Transfer Conf., San Francisco, vol. 5, 1986, pp. 2861–2865.
[7] L. Cheng, G. Xia, Experimental study of CHF in a vertical spirally internally ribbed tube under the condition of high pressure, Int. J. Therm. Sci. 41 (2002) 396–400.
[8] L. Cheng, G. Xia, Critical heat flux in a uniformly heated vertical spirally internally ribbed tube under a wide range of high pressure, in: Proc. 34th. National Heat Transfer Conf., Pittsburgh, August, 2000, pp. 20–22.
[9] G.D Zarnett, M.E. Charles, Cocurrent gas–liquid flow in horizontal tubes with internal spiral ribs, Can. J. Chem. Eng. 47 (1969) 238.
[10] J. Weisman, J. Lan, P. Disimile, Two-phase (air–water) flow patterns and pressure drop in the presence of helical wire ribs, Int. J. Mulitiphase Flow 20 (5) (1994) 885–899.
[11] G.B. Watson et al., Critical heat flux in inclined vertical smooth and ribbed tubes, in: Proc. 5th Engng heat Transfer Conf., Tokyo, Japan, Paper 6.8, Japanese Society of Mechanical Engineering, 1974.
[12] Y. Katto, A generalized correlation of critical heat flux for the forced convective boiling in vertical uniformly heated round tubes, Int. J. Heat Mass Transfer (21) (1978) 1527–1542.
[13] R.M. Tain, S.C. Cheng, Critical heat flux measurements in a round tube for CFCs and CFC alternatives, Int. J. Heat Mass Transfer 36 (1993) 2039–2049.
[14] Y. Katto, On the heat flux/exit-quality type correlation of the CHF of forced convective boiling in uniformly heated round tubes, Int. J. Heat Mass Transfer 24 (1980) 533–539.
[15] I.C. Bang, S.H. Chang, W.P. Paek, Visualization of the subcooled flow boiling of R-134a in a vertical rectangular channel with an electrically heated wall, Int. J. Heat Mass Transfer 47 (2004) 4349–4363.
[16] Research Institute of Shanghai Boiler Works, Experimental investigation on boiler heat transfer characteristics in subcritical pressure once-through boiler, Boiler Tech., No. 9, 1976, pp. 16–33.
[17] R.W. Bowring, A simple but accurate round tube uniform heat flux, dryout correlation over the pressure range 0.7–17 MN/m2 (100–2500 psia), AEEW-R 789, 1972.
[18] Y. Katto, H. Ohno, An improved version of the generalized correlation of critical heat flux for the forced convective boiling in uniformly heated vertical tubes, Int. J. Heat Mass Transfer 27 (1984) 1641–1648.